Energy Conversion and Management 49 (2008) 2055–2062

Contents lists available at ScienceDirect

Energy Conversion and Management

journal homepage: www.elsevier.com/locate/enconman

Preparation, thermal and flammability properties of a novel form-stable phase change materials based on high density polyethylene/poly(ethylene-co-vinyl acetate)/organophilic montmorillonite nanocomposites/paraffin compounds

Yibing Cai [a,b], Lei Song [a,*], Qingliang He [a], Dandan Yang [a], Yuan Hu [a]

[a] State Key Laboratory of Fire Science, University of Science and Technology of China, Hefei, Anhui 230027, People's Republic of China
[b] Key Laboratory of Eco-textiles, Ministry of Education, Jiangnan University, Wuxi, Jiangsu 214122, People's Republic of China

ARTICLE INFO

Article history:
Received 4 July 2007
Accepted 25 February 2008
Available online 18 April 2008

Keywords:
Phase change materials (PCM)
Organophilic montmorillonite (OMT)
Thermal stability
Latent heat
Flammability

ABSTRACT

The paraffin is one of important thermal energy storage materials with many desirable characteristics (i.e., high heat of fusion, varied phase change temperature, negligible supercooling, self-nucleating, no phase segregation and cheap, etc.), but has low thermal stability and flammable. Hence, a novel form-stable phase change materials (PCM) based on high density polyethylene (HDPE)/poly(ethylene-co-vinyl acetate) (EVA)/organophilic montmorillonite (OMT) nanocomposites and paraffin are prepared by twin-screw extruder technique. The structures of the HDPE–EVA/OMT nanocomposites and the form-stable PCM are evidenced by the X-ray diffraction (XRD), transmission electronic microscopy (TEM) and scanning electronic microscope (SEM). The results of XRD and TEM show that the HDPE–EVA/OMT nanocomposites form the ordered intercalated nanomorphology. The form-stable PCM consists of the paraffin, which acts as a dispersed phase change material and the HDPE–EVA/OMT nanocomposites, which acts as the supporting material. The paraffin disperses in the three-dimensional net structure formed by HDPE–EVA/OMT nanocomposites. The thermal stability, latent heat and flammability properties are characterized by thermogravimetry analysis (TGA), dynamic Fourier-transform infrared (FTIR), differential scanning calorimeter (DSC) and cone calorimeter, respectively. The TGA and dynamic FTIR analyses indicate that the incorporation of suitable amount of OMT into the form-stable PCM increase the thermal stability. The DSC results show that the latent heat of the form-stable PCM has a certain degree decrease. The cone calorimeter shows that the heat release rate (HRR) has remarkably decreases with loading of OMT in the form-stable PCM, contributing to the improved flammability properties.

1. Introduction

Energy needs for a wide variety of applications were depended on time and some energy resources. Therefore, the storage of energy was necessary to meet these energy needs. Among the different methods of thermal energy storage, the latent energy storage was a particularly attractive technique, since it provided a high energy storage density and had the capacity to store heat as latent heat of fusion at a constant temperature corresponding to the phase transition temperature of the phase change materials (PCM). The applications of the PCM were very extensive, such as wall [1], gypsum board [2], concrete [3–6] and floor [7]. The results showed that the building materials with PCM could provide the constantly indoor temperature and comfortably livings environments. Much attention had been paid to the form-stable PCM, which represented a rational alternative to traditional PCM. Among the various kinds of PCM of interest, paraffin had been found to exhibit many desirable characteristics, such as high heat of fusion, varied phase change temperature, negligible supercooling, lower vapor pressure in the melt, chemically inert and stable, self-nucleating, no phase segregation and commercial availability at reasonable cost [8,9].

In recent years, many literatures had reported the preparation, physical and chemical properties of the form-stable PCM based on paraffin. Lee and Choi [10] studied the durability of HDPE/paraffin blends as energy storage materials by investigation of the seepage behavior of paraffin. The results showed that the total stored energy was comparable with that of the traditional PCM. Ye and Ge [11] prepared a PE/paraffin compound (PPC) acting as a form-stable PCM. They recommended that the form-stable PCM containing 75 wt% paraffin was a desirable one for application in low temperature heat storage, since it was cheap and easy to be prepared and its latent heat could be comparable with traditional PCM.

Meanwhile, the thermal conductivity was also an important parameter for the practical application of the form-stable PCM.

* Corresponding author. Tel.: +86 551 3607643; fax: +86 551 3601664.
E-mail address: leisong@ustc.edu.cn (L. Song).

0196-8904/$ - see front matter © 2008 Elsevier Ltd. All rights reserved.
doi:10.1016/j.enconman.2008.02.013

Many ways had been studied to enhance the thermal conductivity property of the form-stable PCM. Sari [12] had prepared compounds with two different types of paraffin (T_m = 42–44 °C and 56–58 °C) and HDPE acting as form-stable solid–liquid phase change materials. The thermal conductivity of the form-stable P1/HDPE and P2/HDPE composites was increased, respectively, about 14% and 24% by the addition of expanded graphite (EG) as little as 3 wt%. Xiao et al. [13,14] prepared a shape-stabilized PCM by composing paraffin with a thermoplastic-elastomer poly (styrene–butadiene–styrene) and established its thermal performance during the melting and solidification processes. They concluded that the shape-stabilized PCM exhibited the same phase transition characteristics of paraffin and could be up to 80% of the latent heat of paraffin. And the thermal conductivity of shape-stabilized PCM was increased significantly by introducing EG. Moreover, Zhang et al. [15,16] improved the thermal conductivity of the shape-stabilized PCM by adding some high thermal conductivity solid powers, such as diatomite, wollastonite, organic bentonite, $CaCO_3$ and graphite. The theoretical models (a cubic additive model and a spherical model) predicted well the effective thermal conductivity property. Zhang et al. [17] prepared the paraffin/expanded graphite composite phase change thermal storage material with a large thermal storage capacity, improved thermal conductivity and no liquid leakage during its solid–liquid phase change. Liu et al. [18] encapsulated the form-stable PCM with an inorganic silica gel polymer and study the hydrophilic–lipophilic properties. The results indicate that the enthalpy of the microencapsulated PCM was reduced little, while their hydrophilic properties were enhanced largely. However, the studies of the thermal stability and flammability properties of the form-stable PCM were rare and influenced severely the application in buildings. Therefore, it was significant to enhance thermal and flammability properties of the form-stable PCM.

Based on the above literature survey, it was worthwhile to note that the form-stable PCM acted a direct heat storage medium. And it can be made into granular material with desirable dimensions. In our previous work [19,20], we had investigated combustion characteristics of form-stable PCM with different flame retardant systems. It has been found that the intumescent flame retardant (IFR) was optimum and environmental flame retardant system. Meanwhile, the synergistic effect between IFR and OMT in the form-stable PCM was also studied. The results showed that the loading of OMT caused to a significant decrease of the HRR, contributing to the improved flammability. Clay fillers could become a popular "green" alternative to current flame-retardant additives for polymer and nanoclay will act as an interfacial agent in the multiphase polymer blends. The polymer/clay nanocomposites have superior mechanical, thermal stability, flame retardancy, dimensional and barrier performances. Therefore, in this paper, the objective of the study will introduce nanocomposite technology into the PCM and prepare the novel form-stable PCM based on the HDPE–EVA/OMT nanocomposites (supported material) and the paraffin (dispersed phase change material) compounds. The aim is in order to improve the thermal stability and flame retardant properties of the form-stable PCM, and thus apply best in buildings. The results show that the incorporation of OMT improves notably the thermal stability and flammability properties of the form-stable PCM.

2. Experiments

2.1. Materials

The HDPE and EVA (containing 18 wt% vinyl acetate) were supplied as pellets by Daqing Petrochemical Company, ChinaPetroleum and Beijing Petrochemical, respectively. Paraffin was available commercially with melting temperature (T_m = 56–60 °C) and latent heat of 167.03 kJ/kg. The organophilic montmorillonite (OMT) was kindly provided by the Keyan Chemical Company.

2.2. Formation of the HDPE–EVA/OMT nanocomposites and the form-stable PCM

The HDPE, EVA and desired amounts of OMT were premixed in high-speed blender for 10 min. The ratio of HDPE/EVA was fixed as 75/25 by weight and the detailed mass ratio of HDEP/EVA and OMT was listed in Table 1. Then the mixture was extruded at 180 °C using a twin-screw extruder (TE-35, KeYa, China). The extruded strands were pelletized, dried at 80 °C, and yielded finally the HDPE–EVA/OMT nanocomposites.

Then, the form-stable PCM with the aforementionedly resulting pellets and paraffin were premixed and prepared by using a twin-screw extruder. The temperature range and the screw speed of the twin-screw extruder were set at 120–170 °C and 450 rpm, respectively. The detailed compositions of the form-stable PCM were listed in Table 1.

2.3. Characterization

X-ray diffraction (XRD) experiments were performed directly on the samples using a Japan Rigaku D/max-rA X-ray diffractometer (30 kV, 10 mA) with Cu Kα (λ = 1.54178 Å) irradiation at a rate of 2°/min in the range of 1.5–10°.

Transmission electronic microscopy (TEM) images were obtained on a Jeol JEM-100SX transmission electron microscope with an acceleration voltage of 100 kV. The HDPE–EVA/OMT nanocomposites specimen was cut at room temperature using an ultramicrotome (Ultracut-1, UK) with a diamond knife from an epoxy block with the films of the nanocomposites embedded.

Scanning electronic microscope (SEM) observations were performed for the form-stable PCM. The form-stable PCM specimens were broken in liquid nitrogen and the fractured surfaces were coated by gold before SEM investigations. SEM images were obtained on a PHILIPS XL30ESEM microscope.

Thermogravimetry analyses (TGA) were conducted with a NETZSCH STA409C Thermal Analyzer instrument. In each case, the 10 mg specimens were heated from 25 to 800 °C with a linear heating rate of 10 °C/min under N_2 atmosphere.

The Fourier-transfer infrared (FTIR) spectra were scanned using a Nicolet MAGNA-IR 750 spectrometer for characterization of the form-stable PCM at room temperature. Dynamic Fourier-transform infrared (FTIR) spectra were recorded using a Nicolet MAGNA-IR 750 spectrophotometer equipped with a ventilated oven having a heating device. The film samples were placed in a ventilated oven at a heating rate of 10 °C/min for the dynamic measurement of FTIR spectra in the condensed phase during the thermo-oxidative degradation. The intensity of peaks is expressed in terms of area of the peaks. The area of the peaks at 20 °C is used as a standard (100%). The intensity of peaks at higher temperature is evaluated relative to the intensity of peaks at 20 °C.

Differential scanning calorimeter (DSC) was carried out in a nitrogen atmosphere by means of Perkin–Elmer Diamond DSC

Table 1
Samples identification and compositions

Samples	Compositions
PCM1	Paraffin75 wt% + HDPE–EVA25 wt%
PCM2	Paraffin75 wt% + HDPE–EVA22.5 wt% + OMT2.5 wt%
PCM3	Paraffin75 wt% + HDPE–EVA20 wt% + OMT5 wt%
PCM4	Paraffin75 wt% + HDPE–EVA15 wt% + OMT10 wt%

thermal analyzer from 20 to 200 °C with a linear heating rate of 5 °C/min. The nitrogen flow rate was 20 ml/min. The precision on calorimeter and temperature measurements are ±2.0% and ±2.0 °C, respectively. Indium was used as a reference for temperature calibration. Samples were measured in a sealed aluminum pan with a mass of about 5.0 mg. The latent heat was calculated as the total area under the peaks of solid–solid and solid–liquid transitions of the paraffin in the form-stable PCM by thermal analysis software.

Flammability property was characterized by cone calorimeter. The signals from the cone calorimeter were recorded and analyzed by a computer system. All samples ($100 \times 100 \times 3$ mm^3) were examined in a Stanton Redcroft cone calorimeter according to ISO5660 under a heat flux of 35 kW/m^2. Exhaust flow rate was 24 L/s and the spark was continued until the sample ignited. The typical results from cone calorimeter were reproducible to within ±10%.

3. Results and discussion

3.1. Dispersibility of HDPE–EVA/OMT nanocomposites and the corresponding form-stable PCM

The XRD patterns of (a) MMT, (b) OMT (c) HDPE–EVA/OMT (5 wt%) nanocomposites, (d) PCM3 and (e) PCM4 are shown in Fig. 1. The peaks correspond to the (001) plane reflection of the clays. The average basal spacing of OMT increases from 1.5 nm of original MMT to 2.4 nm. The increased spacing suggests the chains of hexadecyl trimethyl ammonium bromide (C16) intercalate into the gallery of MMT and expand it. The intercalated morphology of HDPE–EVA/OMT (5 wt%) nanocomposites (Fig. 1c) is proved by the interlayer spacing, which is derived from the d_{001} peak of montmorillonite and is increased from 2.4 nm for OMT (Fig. 1b) to 3.8 nm. The 1.4 nm galley height increase indicates the intercalated nanostructure has been formed. The basal spacing of PCM3 (Fig. 1d) and PCM4 (Fig. 1e) is 3.9 nm, which has a 1.5 nm gallery height increase compared with OMT. However, the diffraction peak intensity of the form-stable PCM is evidently stronger than that of the HDPE–EVA/OMT (5 wt%) nanocomposites. The reasons may have two aspects. Firstly, the morphology of the HDPE–EVA/OMT (5 wt%) nanocomposites is an intercalated-delaminated structure, which leads to the width of peak. Secondly, the OMT itself is also a kind of supporting material [21]. The paraffin could intercalate partly into the silicate layers of OMT during the melt-mixing process. The similar results have been reported in another study [20].

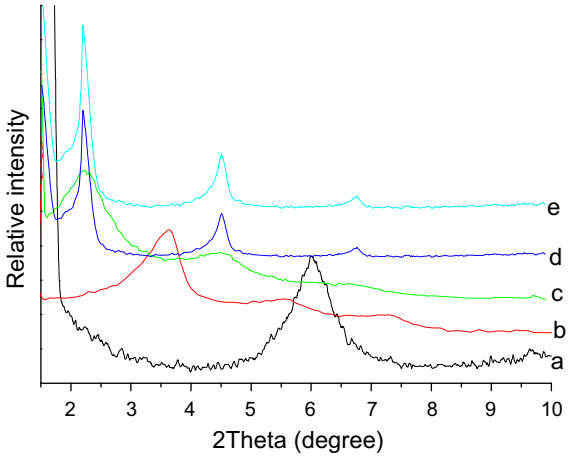

Fig. 1. XRD patterns of (a) MMT, (b) OMT, (c) HDPE–EVA/OMT (5 wt%) nanocomposites, (d) PCM3 and (e) PCM4.

Fig. 2 demonstrates the TEM microscopy of HDPE–EVA/OMT (5 wt%) nanocomposites. Homogenous and ordered dispersion of the individual clay layers and the tactoids throughout the HDPE/EVA blend are observed. The reasons include several aspects. Firstly, the vinyl acetate (VA) groups in the EVA chains promote the interaction with clay layers by penetration of the EVA chains into the clay galleries. Secondly, the EVA acts as a reactive compatibilizer and improves the interfacial function between HDPE and OMT. And the EVA is more polar, leading to the silicate clay migrate more towards to the EVA phase. Thirdly, the clay acts as an interfacial agent for polymer blends system [22–26], the intercalated silicate layers are pushed towards the interphase due to the common intercalation and are shared by the two polymers, which lead to a reduction in interfacial tension. Meanwhile, HDPE is compatible with EVA in the amorphous region, which leads to a good dispersion of the clay in the matrix [27].

The morphology of the form-stable PCM are investigated by SEM. The images of PCM1, PCM2, PCM3 and PCM4 are shown in Fig. 3. SEM studies show that the HDPE–EVA alloy can contain commendably the paraffin and form compact three-dimensional net structure. The paraffin is well dispersed in the HDPE–EVA alloy. Meanwhile, the OMT acts as an interfacial modifier for polymer blend and itself is also a kind of supporting material [21]. So the additive of OMT makes the coalescent more compact between the HDPE–EVA alloy and the paraffin.

3.2. FTIR characterization

Fig. 4 displays the FTIR spectra of form-stable PCM1 and PCM3. Both the form-stable PCM1 and PCM3 have the characteristic bands: 2917 cm^{-1}, 2850 cm^{-1}, 1741 cm^{-1}, 1634 cm^{-1}, 1468 cm^{-1}, 1380 cm^{-1}, 1240 cm^{-1} and 719 cm^{-1}. The assignments of the main peaks of FTIR spectra are listed in Table 2. Besides these bands, the form-stable PCM3 also has the characteristic bands of montmorillonite: 1033 cm^{-1}, 520 cm^{-1}, 465 cm^{-1}, corresponding to the stretching vibration of Si–O–Si, the stretching vibration of Al–O and Si–O bending vibration of montmorillonite, respectively. The result shows that the HDPE–EVA/OMT nanocomposites is formed.

3.3. Thermal degradation stability of the form-stable PCM

Clay layers have good barrier action, which can improve the thermal stability of polymer/clay nanocomposites. On the other hand, the alkylammonium cations in the organophilic montmorillonite could suffer decomposition following the Hofmann elimination reaction [28,29], and its product would catalyse the degradation of polymer matrixes. Thirdly, the clay itself can also catalyse the degradation of polymer matrixes. The latter two ac-

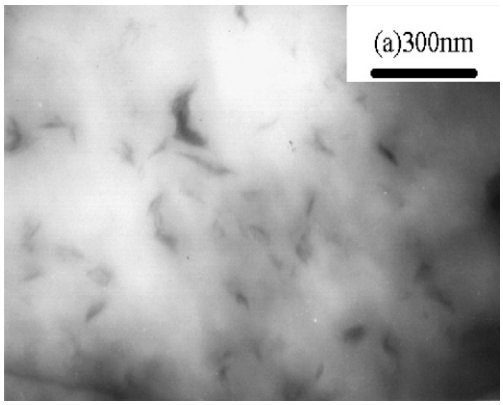

Fig. 2. TEM micrographs of HDPE–EVA/OMT (5 wt%) nanocomposites.

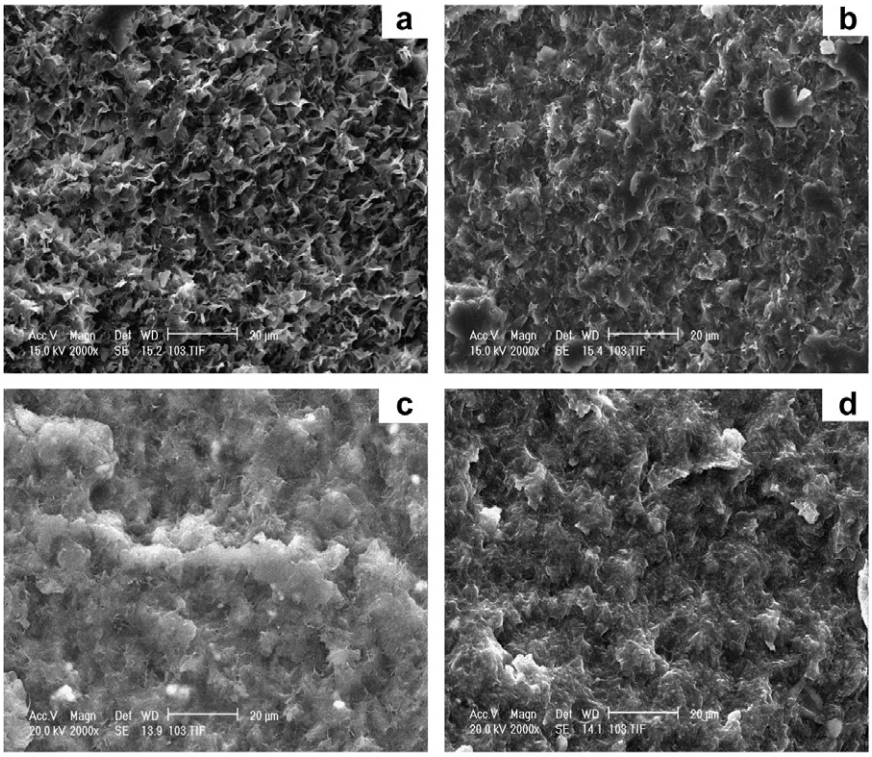

Fig. 3. The SEM images of the (a) PCM1, (b) PCM2, (c) PCM3 and (d) PCM4.

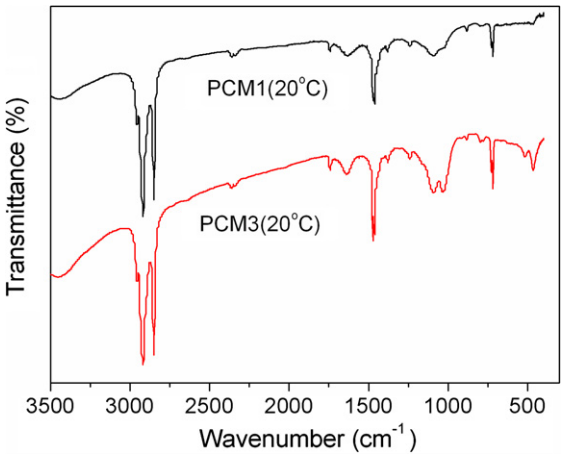

Fig. 4. FTIR curves for the form-stable PCM1 and PCM3 at room temperature.

Table 2
FTIR band assignments of the form-stable PCM1 and PCM3

Absorption peak (cm^{-1})	Band assignment
2917	Asymmetric stretching vibration of C–H
2850	Symmetric stretching vibration of C–H
1741	Stretching vibration of C=O
1634	Stretching vibration of C=C
1468	CH_2or CH_3 deformation vibration
1380	CH_3 (end-group)
1240	C–O stretching vibration
1033	Si–O–Si stretching vibration of montmorillonite
719	CH_2 rocking vibration of $(CH_2)_n$, $n \geqslant 4$
520	Al–O stretching vibration of montmorillonite
465	Si–O bending vibration of montmorillonite

tions would reduce the thermal stability of polymer/clay nanocomposites [30]. Thermal degradation stability is an important property for which the polymer/clay nanocomposite plays an important role. The TGA data corresponding to the 5 wt% loss temperature ($T_{-5\,wt\%}$), the maximum temperature of mass loss (T_{max1} and T_{max2}) obtained from the DTGA curves are listed in Table 3. In this article, only DTGA curves for the form-stable PCM are presented (Fig. 5).

Fig. 5 shows that the maximum mass loss temperatures of the form-stable PCM. The DTGA curves display a two-stage thermal degradation process for the form-stable PCM. The first step is roughly from 200 to 450 °C, corresponding to the degradation of the deacylation reactions of the poly(ethylene-co-vinyl acetate) (EVA), paraffin molecular chain and surfactant molecule (C16) coming from the Hofmann elimination reaction [28,29]. The $T_{-5\,wt\%}$ degradation temperature and the maximum loss temperature (T_{max1}) of the form-stable PCM containing OMT are higher than those of the HDPE–EVA/paraffin compound (PCM1). This may be attributed to the nano-dispersed silicate layers, which can slow the decomposition and increase the temperature of degradation by acting as an excellent thermal insulator and mass transport barrier. At the same time, the $T_{-5\,wt\%}$ and the T_{max1} of the form-stable PCM decrease slightly with increasing OMT loading. The reason may be that the lewis or Bronsted acid sited in the clay layers generates at 200 °C according to the Hofmann degradation mechanism for OMT which has a catalyst effect on the deacylation of EVA [27].

Table 3
TGA data of the form-stable PCMs

Samples	$T_{-5\,wt\%}$ (°C)	T_{max1} (°C)	T_{max2} (°C)	Residue (800 °C)
PCM1	270.1	359.6	473.7	1.33
PCM2	290.3	373.0	476.6	3.93
PCM3	287.8	378.4	465.5	5.06
PCM4	281.7	368.8	459.0	15.26

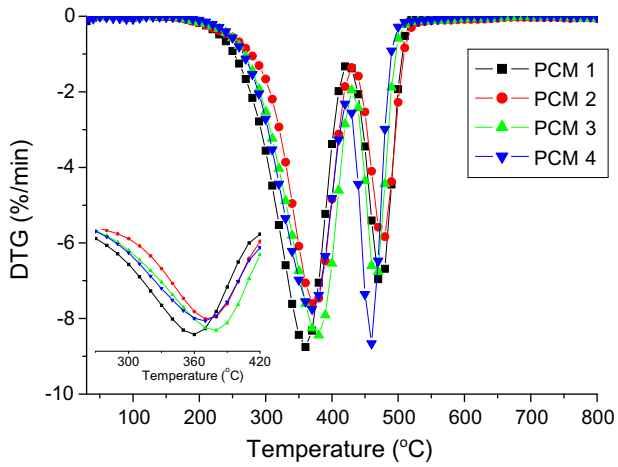

Fig. 5. DTGA curves of the form-stable PCM.

The second step is about from 450 to 500 °C. It may be assigned to the degradation of the HDPE and the backbone of the EVA, which formed in the first step. On elevating the temperature above 450 °C, thermal stability of the form-stable PCM in the second stage does not vary significantly from that of the PCM1. The charred residue of the form-stable PCM at 800 °C is simultaneously listed in Table 3. The charred residue amount increases in the order of PCM4 > PCM3 > PCM2 > PCM1. The char residue amount of the form-stable PCM with OMT is notably higher than that of PCM1, probably because the OMT is more advantageous to form high-performance carbonaceous-silicate charred layer building up on the surface which insulates the underlying material and slows the escape of the volatile products generated during thermal degradation, The results explain the enhancement of thermal stability of the form-stable PCM compared with HDPE–EVA/paraffin compound.

In summary, the OMT has two opposing functions in the thermal stability of the polymer/clay nanocomposites. One is its barrier effect, which should improve the thermal stability, and the other is the catalysis effect towards the degradation of the polymer matrix, which would decrease the thermal stability. Adding a low fraction to the polymer matrix, the clay layers should be well dispersed and the barrier effect is predominant. But with increasing clay loading, the catalyzing effect rapidly rises and becomes dominant so that the thermal stability of the nanocomposites decreases [30].

3.4. Thermo-oxidative degradation of the form-stable PCM

Thermo-oxidative degradation (TOD) of the form-stable PCM is investigated by dynamic FTIR. The changes of C–H absorption intensities of aliphatic groups in the 2500–3200 cm^{-1} regions are generally used to evaluate the thermal stability of polymers during TOD studies [31]. Fig. 6 presents the dynamic FTIR spectra obtained from the PCM1 (Fig. 6A) and PCM3 (Fig. 6B) at different pyrolysis temperatures. The important absorption peaks at 2917 cm^{-1} and 2850 cm^{-1} are the characteristic bands of the $-CH_2$ asymmetric and symmetric vibrations, respectively. The relative intensity of the $-CH_2$ absorption peaks decrease with the increasing temperature. The changes of the relative intensities are presented in Table 4. It can be seen that the relative peak intensities of the PCM3 are much higher than that of the PCM1 at the same temperature, revealing that the incorporation of OMT increase the thermo-oxidative degradation stability of the main chains than that of the HDPE–EVA/paraffin compound (PCM1).

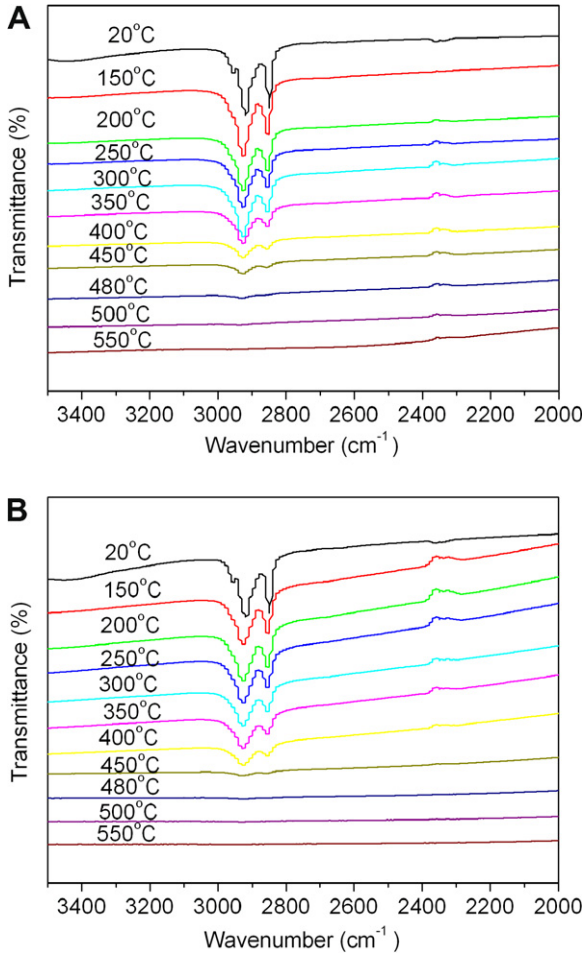

Fig. 6. Dynamic FTIR spectra at different pyrolysis temperature: (A) PCM1 and (B) PCM3.

Table 4
Effect of pyrolysis temperature on the relative intensities (%) of peaks (2917 cm^{-1} and 2850 cm^{-1}) of the form-stable PCM1 and PCM3

Temperature (°C)	Sample PCM1	Sample PCM3
20	100	100
150	86.7	92.5
200	79.8	84.4
250	72.5	76.1
300	61.6	64.4
350	52.0	53.2
400	42.0	43.8
450	26.1	32.5
480	10.5	23.6
500	4.95	11.5
520	2.16	6.38
550	0	2.45

3.5. Latent heat of the form-stable PCM

The typical DSC curves of the paraffin, HDPE and the corresponding form-stable PCM are presented in Fig. 7. The DSC curves show that the paraffin has two phase change peaks. The first minor peak at the left about 42 °C corresponds to the solid–solid phase transition of the paraffin and the second sharp or main peak corresponding to 58 °C represents the solid–liquid phase change of the paraffin. At the same time, the molten peak of HDPE also occurs at around 127 °C. Fig. 7 shows that the phase change peaks of the paraffin are still existence in the form-stable PCM. This is be-

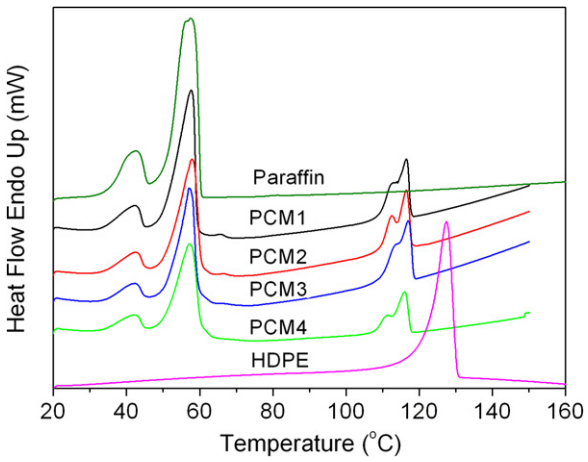

Fig. 7. The DSC curves of the HDPE, paraffin and the corresponding form-stable PCM.

cause the paraffin is a homologous compound of HDPE and there is no chemical reaction among the paraffin, HDPE–EVA and OMT during the preparation of the form-stable PCM. However, the phase change peaks of the paraffin are weaker than the pure paraffin, probably because the three-dimensional net structure partly confines the molecule heat movement of paraffin in the phase change temperature range. It is easy to find that the melting peak of the HDPE is ahead of schedule comparing to the pure HDPE. The main reasons have two aspects. On the one hand, the HDPE and EVA, OMT form polymer alloy nanocomposites. On the other hand, the HDPE and paraffin form polymer alloy in the form-stable PCM. The above two reasons reduce the melting temperature of HDPE. The similar results have also been investigated in the literature [11,19,20].

In Table 5, the thermal properties of the pure paraffin and form-stable PCM, such as transition temperature (T_t), melting temperature (T_m) and the latent heat obtained through the DSC measurement are given. As indicated in Table 5, the T_t and T_m values for both the form-stable PCM approach those of the pure paraffin. However, the latent heat values of the paraffin decrease markedly compared to the pure paraffin. The latent heat of both form-stable PCM should be 125.27 kJ/kg by multiplying the latent heat of the dispersed paraffin (167.03 kJ/kg) with its mass fractions (75 wt%). It may be that the three-dimensional net structure confines the molecule heat movement of paraffin in form-stable PCM and the paraffin partly intercalates the interlayer of the organophilic montmorillonite (OMT). Furthermore, the latent heat of the paraffin dispersed in form-stable PCM decreases with the increase of the OMT amount. The reasons may be that a great deal of paraffin molecular intercalates into the interlay of the excessive OMT, thereby confining the release of the latent heat during the phase change temperature. Although the latent heat of the form-stable PCM has a certain degree decrease, their thermal stability has marked enhancements.

Table 5
Latent heat of the paraffin and the form-stable PCMs

Samples	T_t (°C)	T_m (°C)	Latent heat (kJ/kg)
Paraffin	42.35	57.59	167.03
PCM1	42.33	57.65	111.52
PCM2	42.34	57.92	99.78
PCM3	41.90	57.13	97.21
PCM4	42.04	57.33	91.66

In addition, it is observed that liquid leakage does not occur while the form-stable PCM are performing the phase change from solid to liquid, owing to the fact that the paraffin is dispersed in the formed three-dimensional network structure of the HDPE–EVA/OMT nanocomposites. The similar results are also investigated in the other literatures [11,12,17,19,20].

3.6. Flammability properties

Cone calorimeter is one of the most effective bench-scale methods for studying the flammability properties of materials. Cone calorimeter investigations can be used as a universal approach to ranking and comparing the fire behavior of materials. Therefore, it is not surprising that the cone calorimeter is finding increasing implementation as a characterization tool in research and development of fire retardant polymer materials. Heat release rate, in particular peak HRR, has been found to be the most important parameter to evaluate fire safety [19,20,32].

The heat release rate (HRR) plots for the HDPE–EVA/paraffin compound and the HDPE–EVA/OMT/paraffin compounds with different OMT loading at a heat flux of 35 kW/m^2 are shown in Fig. 8. The peak HRR values (PHRR) are 1573.18 kW/m^2 (PCM1), 1378.30 kW/m^2 (PCM2), 1031.28 kW/m^2 (PCM3) and 920.52 kW/m^2 (PCM4), respectively. The results show that the PHRR have remarkably decreases with the increase of the OMT loading. The PHRR of the HDPE–EVA/OMT/paraffin compounds with 5 wt% and 10 wt% OMT loadings are decreased by about 34.4% (PCM3) and 41.5% (PCM4) compared with that of HDPE–EVA/paraffin compound (PCM1). Gilman [32] reports that the reduction of the HRR peak is a typical feature of polymer layered silicate hybrid, the lower flammability of polymer/clay hybrids is not due to retention of a large fraction of flammable molecules but in the form of carbonaceous char in the condensed phase. The improved flammability properties may be that the ablative reassembling of the silicate layers may occur on the surface of the burning hybrid, creating a physical protective barrier on the surface of the materials during combustion. The reassembling layers would act as a protective barrier and thus limit oxygen diffusion to the substrate and retard the volatilization of the flammable decomposition products [20,33]. Fig. 9 is digital photos for the residues of the form-stable PCM after combustion by cone calorimeter tests. The results show that the HDPE–EVA/paraffin compound (PCM1) is almost burnt out but for the HDPE–EVA/OMT/paraffin compounds a thick, intact charred layer is formed. It can be seen from Fig. 9 that the charred layer is tigh-

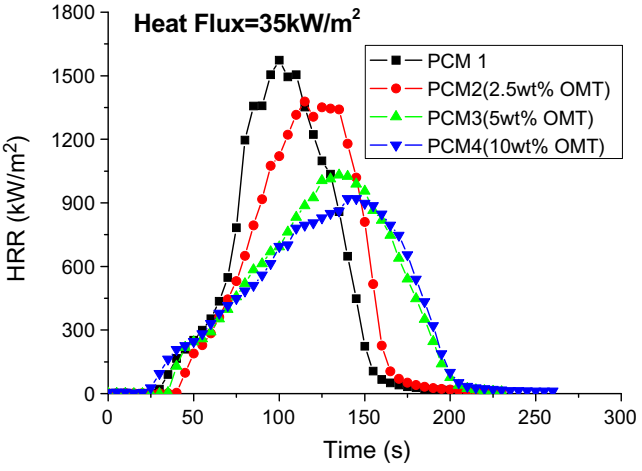

Fig. 8. Heat release rate (HRR) curves of the form-stable PCM.

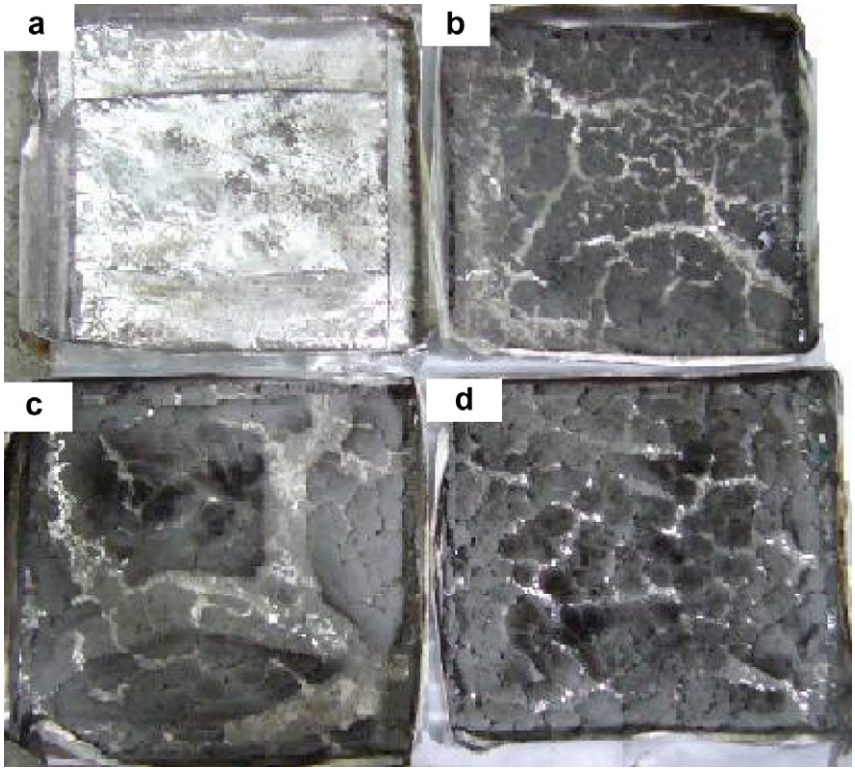

Fig. 9. Digital photos of the residues after combustion: (a) PCM1, (b) PCM2, (c) PCM3 and (d) PCM4.

ter and denser with the increase of OMT loadings, contributing to the barrier property of the silicate clay. Meanwhile, the ablative reassembling of the silicate layers may occur on the surface of the burning hybrid, creating a physical protective barrier on the surface of the materials during combustion [20]. The strong charred layers increase the flammability property of the form-stable PCM.

4. Conclusion

The compounds based on the HDPE–EVA/OMT nanocomposites and paraffin, which acting as a novel form-stable phase change materials (PCM) are prepared by twin-screw extruder technique. The results of XRD and TEM show that the HDPE–EVA/OMT nanocomposites form the ordered intercalated nanomorphology. The SEM analysis indicates that the form-stable PCM is made of the paraffin (a dispersed phase change material) and the HDPE–EVA/OMT nanocomposites (a supporting material). The paraffin disperses in the three-dimensional net structure formed by HDPE–EVA/OMT nanocomposites. The DSC results show that the latent heat of the form-stable PCM has a certain degree decrease. The reasons may be that the three-dimensional net structure and the silicate layers of the OMT confine partly the molecular heat movement of paraffin in form-stable PCM. The TGA and dynamic FTIR analyses indicate that the incorporation of suitable amount of OMT into form-stable PCM increases the thermal stability. Both the $T_{-5\,wt\%}$ of the form-stable PCM with 2.5 wt% OMT and the T_{max1} of the form-stable PCM containing 5 wt% OMT have about 20 °C enhancements compared to the HDPE–EVA/paraffin compound, contributing to the barrier effect of silicate layers. And with the loading of OMT, the charred residue amount has remarkably improvement, which is another reason for the higher thermal stability. It is noteworthy that the physical–chemical effect between the polymer matrix and the OMT has an important role in the thermal degradation process. The cone calorimeter indicates that the PHRR have remarkably decreases with the increasing loading of OMT, contributing to the improved flammability properties.

Acknowledgements

The work was financially supported by the National Natural Science Foundation of China (No. 50476026), Specialized Research Fund for the Doctoral Program of Higher Education (20040358056), Program for New Century Excellent Talents in University and Program of Jiangnan University (No. 206000–21050737).

References

[1] Rudd AF. Phase change material wall for distributed thermal storage in building. ASHRAE Trans 1993;99:339–44.
[2] Feldman D, Banu D, Hawes D. Low chain esters of stearic-acid as phase change materials for thermal-energy storage in buildings. Sol Energy Mater Sol Cells 1995;36(3):311–22.
[3] Lane GA. Solar heat storage latent heat material, vol. 12. Boca Raton: CRC Press, Inc.; 1986. p. 50–65.
[4] Hawes DW, Feldman D. Absorption of phase-change materials in concrete. Sol Energy Mater Sol Cells 1992;27(2):91–101.
[5] Hadjieva M, Stoykov R, Filipova T. Composite salt–hydrate concrete system for building energy storage. Renew Energy 2000;19(1–2):111–5.
[6] Lee T, Hawes DW, Banu D. Control aspects of latent heat storage and recovery in concrete. Sol Energy Mater Sol Cells 2000;62(3):217–37.
[7] Farid M, Kong WJ. Under floor with latent heat storage. Proc Inst Mech Eng A 2001;215:601–9.
[8] Hasnain SM. Review on sustainable thermal energy storage technologies, part I: heat storage materials and techniques. Energy Convers Manage 1998;39(11):1127–38.
[9] Peng S, Fuchs A. Polymeric phase change composites for thermal energy storage. J Appl Polym Sci 2004;93:1240–51.
[10] Lee CH, Choi HK. Crystalline morphology in high-density polyethylene/paraffin blend for thermal energy storage. Polym Compos 1998;19:704–8.
[11] Ye H, Ge XS. Preparation of polyethylene–paraffin compound as a form-stable solid–liquid phase change material. Sol Energy Mater Sol Cells 2000;64:37–44.
[12] Sari A. Form-stable paraffin/high density polyethylene composites as solid–liquid phase change materials for thermal energy storage: preparation and thermal properties. Energy Convers Manage 2004;45:2033–42.

[13] Xiao M, Feng B, Gong KC. Preparation and performance of shape stabilized phase change thermal storage materials with high thermal conductivity. Energy Convers Manage 2002;43:103–8.
[14] Xiao M, Feng B, Gong KC. Thermal performance of a high conductive shape-stabilized thermal storage material. Sol Energy Mater Sol Cells 2001;69:293–6.
[15] Zhang YP, Ding JH, Wang X, Yang R, Lin KP. Influence of additives on thermal conductivity of shape-stabilized phase change material. Sol Energy Mater Sol Cells 2006;90:1692–702.
[16] Zhang YP, Yang R, Di HF. Preparation, thermal performance and application of shape-stabilized PCM in energy efficient buildings. In: Collection of technical papers – 2nd international energy conversion engineering conference; 2004. p. 600–610.
[17] Zhang ZG, Fang XM. Study on paraffin/expanded graphite composite phase change thermal energy storage material. Energy Convers Manage 2006;47:303–10.
[18] Liu X, Liu HY, Wang SJ, Zhang L, Cheng H. Preparation and thermal properties of form stable paraffin phase change material encapsulation. Energy Convers Manage 2006;47:2515–22.
[19] Cai YB, Hu Y, Song L, Tang Y. Flammability and thermal properties of high density polyethylene/paraffin hybrid as a form-stable phase change material. J Appl Polym Sci 2006;99:1320–7.
[20] Cai YB, Hu Y, Song L, Kong QH. Preparation and flammability of high density polyethylene/paraffin/organophilic montmorillonite hybrids as a form-stable phase change material. Energy Convers Manage 2007;48:462–9.
[21] Fang XM, Zhang ZG. A novel montmorillonite-based composites phase change material and its applications in thermal storage building materials. Energy Buildings 2006;38:377–80.
[22] Voulgaris D, Petridis D. Emulsifying effect of dimethyldioctadecylammonium-hectorite in polystyrene/poly(ethyl methacrylate) blends. Polymer 2002;43:2213–8.
[23] Wang Y, Zhang Q, Fu Q. Compatibilization of immiscible poly(propylene) /polystyrene blends using clay. Macromol Rapid Commun 2003;24: 231–5.
[24] Yurekli K, Karim A, Amis EJ, Krishnamoorti R. Influence of layered silicates on the phase-separated morphology of PS-PVME blends. Macromolecules 2003;36:7256–67.
[25] Ray SS, Pouliot S, Bousmina M, Utracki LA. Role of organically modified layered silicate as an active interfacial modifier in immiscible polystyrene/ polypropylene blends. Polymer 2004;45:8403–13.
[26] Yurekli K, Karim A, Amis EJ, Krishnamoorti R. Phase behavior of PS-PVME nanocomposites. Macromolecules 2004;37:507–15.
[27] Lu HD, Hu Y, Kong QH, Cai YB. Influence of gamma irradiation on high density polyethylene/ethylene-vinyl acetate/clay nanocomposites. Polym Adv Technol 2004;15:601–5.
[28] Zanetti M, Camino G, Thomann R. Synthesis and thermal behaviour of layered silicate–EVA nanocomposites. Polymer 2001;42:4501–7.
[29] Xie W, Gao Z, Pa WP, Hunter D, Singh A, Vaia R. Thermal degradation chemistry of alkyl quaternary ammonium montmorillonite. Chem Mater 2001;13:2979–90.
[30] Zhao CG, Qin HL, Gong FL, Feng M, Zhang SM, Yang MS. Mechanical, thermal and flammability properties of polyethylene/clay nanocomposites. Polym Degrad Stab 2005;87:183–9.
[31] Xie RC, Qu BJ, Hu KL. Dynamic FTIR studies of thermo-oxidation of expandable graphite-based halogen-free flame retardant LLDPE blends. Polym Degrad Stab 2001;72:313–21.
[32] Gilman JW. Flammability and thermal stability studies of polymer layered-silicate (clay) nanocomposites. Appl Clay Sci 1999;15:31–49.
[33] Gilman JW, Kashivagi TCL, Giannelis EP, Manias E, et al. In: Le Bras M, Camino G, Bourbigot S, Delobel R, editors. Fire retardancy of polymer. Cambridge: The Royal Society of Chemistry; 1998. p. 203.